Sigma J Eng & Nat Sci 37 (1), 2019, 93-104

Sigma Journal of Engineering and Natural Sciences
Sigma Mühendislik ve Fen Bilimleri Dergisi

Research Article

DRYING OF OKRA BY INFRARED RADIATION

Seda TANTA[1], İbrahim DOYMAZ*[2]

[1]*Yildiz Technical University, Dept. of Chemical Eng., Esenler-ISTANBUL;* ORCID: 0000-0002-5524-2723
[2]*Yildiz Technical University, Dept. of Chemical Eng., Esenler-ISTANBUL;* ORCID: 0000-0002-4429-6443

Received: 08.12.2018 Revised: 31.12.2018 Accepted: 03.01.2019

ABSTRACT

In this study, we tried to evaluate mass transfer during an infrared drying of okra. Infrared radiation (IR) power (62, 74, 88 and 104 W) as drying parameter is evaluated on drying characteristics of okra. The infrared power affected the drying and colour characteristics of okra. Drying time was found decreasing with increase in infrared power. Four thin-layer drying models were evaluated for moisture ratios using nonlinear regression analysis. The results of regression analysis indicated that the Midilli & Kucuk model gave the excellent fit for the drying data under all drying conditions with the lowest χ^2 and *RMSE* values and highest R^2 value. The effective moisture diffusivity at each infrared power was determined by Fick's second law of diffusion, an increase in the power led to increase in the effective moisture diffusivity between 8.54×10^{-10} and 2.32×10^{-9} m^2/s. The dependence of effective moisture diffusivity on infrared power was expressed by a modified Arrhenius type equation. Activation energy was estimated as 3.91 kW/kg.
Keywords: Activation energy, effective moisture diffusivity, infrared drying, mathematical modelling, okra.

1. INTRODUCTION

Okra (*Abelmoschus esculentus* L.) is a type of annual vegetable crop herbaceous plant, belonging to the Malvaceae family. It probably originates in African region and widely has been grown in Asia, southern Europe and American region [1]. Worldwide production of okra is 8900434 metric ton in 2016, and the major producers include India, Nigeria, Sudan, Mali and Pakistan. Okra is grown on 5742 ha areas in Turkey with a production of 29529 ton in 2016 [2]. Okra is a very good source of protein, vitamin C, vitamin A, vitamin K, thiamine, niacin, riboflavin, foliate, magnesium, potassium, calcium, manganese, dietary fibre and is low in saturated fat. It is consumed in fresh, cooked, canned, pickled, dried, frozen forms and also used as an additive for soups, salads and stews [3]. Okra, like most other fruits and vegetables, is susceptible to rapid deterioration because of their high moisture content. It is preserved in some forms, such as frozen, canned and dried.

Drying is a traditional or industrial food preservation method. The major objective of drying is to reduce water activity of raw materials and extend the self-life. Drying not only reduces the moisture content of products but also alters other physical, chemical, and biological properties, such as antioxidant capacity, enzymatic activity, aroma, flavour and so on [1]. The most conventional method used for drying of agricultural products is hot air drying, which is low-cost

* Corresponding Author: e-mail: doymaz@yildiz.edu.tr, tel: (212) 383 47 48

and easily controlled but low-energy efficiency and lengthy drying time during the last drying stage. In addition, drying process not only consumes great amount of energy, but also could cause some undesirable changes in physical and chemical properties of biological products [4].

By subjecting the material to infrared radiation, the heating power generated can penetrate into the food materials. Infrared radiation has gained popularity because of its superior thermal efficiency and fast response time = drying rate compared to conventional heating. Infrared radiation heating has been widely applied in recent years to different thermal processing systems in the food industry, such as pasteurization, drying, and frying [5]. Infrared drying has gained popularity as an alternative drying method for obtaining high quality dried fruits, vegetables and grains. Some studies have reported on the effects of infrared application and/or by a combined infrared-assisted convection process such as apple [6], pineapple [7], tomato [8], and Jerusalem artichoke [9].

Several researchers in recent times have investigated the drying characteristics or behaviour of okra using different drying methods such as open sun drying [10,11], solar drying [10,12,13], hot-air drying [1,3], heat pump drying [1], vacuum freezing drying [14] and others. However, the infrared drying of okra has not been reported in literature. The objectives of this study were to investigate the effect of infrared power on drying and colour characteristics, fit the experimental data to some thin-layer drying models, and compute effective moisture diffusivity and activation energy of okra.

2. MATERIAL AND METHODS

2.1. Material

Okra (*Abelmoschus esculentus* L.) samples were obtained from a local grower in Istanbul. They were packed into plastic bags and stored in a refrigerator (Arcelik 1050T, Eskisehir, Turkey) at 4°C prior to use. The initial moisture content of okra samples was determined by using an oven at 105°C for 24 h. Triplicate samples were used for the determination of moisture content and the average values were reported as 5.858 kg water/kg dry matter. The okra samples with uniform sizes were manually selected and average length and diameter of selected samples were about 7.5±0.5 cm and 2.0±0.3 cm, respectively. Before experiments, okra samples were taken from refrigerator and brought up to the room temperature. After, tap water was used to remove the surface dirt. Excess water from surface of samples was eliminated with sterile tissue paper.

2.2. Experimental Procedure

Drying experiments were carried out in a moisture analyzer with a 250 W halogen lamp (Snijders Moisture Balance, Snijders b.v., Tilburg, Holland). The experiments were carried out using several infrared power levels such as 62, 74, 88 and 104 W. Before the drying process, the samples were separated evenly and spread homogeneously over the pan. The power level was set from the control unit of the equipment. Approximately 40 g of sample was put into the dryer after weighing. Weight loss was recorded at 15 min intervals during drying. A digital balance (Mettler-Toledo AG, Grefensee, Switzerland, model BB3000) with ±0.1 g accuracy was employed in recording the sample weight. The drying process was continued until the moisture content remaining in the sample was about 0.175±0.02 kg water/kg dry matter. The dried products were cooled, packaged in low-density polyethylene bags and stored in incubators at ambient temperature. The experiments were run in triplicate and the drying curves were plotted using the average values of the moisture content.

2.3. Mathematical Modelling

Four thin-layer drying models were selected to describe the drying kinetics of the samples (Table 1). The moisture content (*M*), moisture ratio (*MR*) and drying rate (*DR*) of okra were calculated using the following equations:

Table 1. Mathematical models applied to the drying curves

Model name	***Model equation***
Henderson & Pabis	$MR = a\,exp(-kt)$
Page	$MR = exp(-kt^n)$
Midilli & Kucuk	$MR = a\,exp(-kt^n) + bt$
Aghbashlo et al.	$MR = \exp\left(-\dfrac{k_1 t}{1 + k_2 t}\right)$

a, k, k_1, k_2 *and n* empirical constants and coefficients in the models

$$M = \frac{W - W_d}{W_d} \tag{1}$$

$$MR = \frac{M_t - M_e}{M_0 - M_e} \tag{2}$$

$$DR = \frac{M_t - M_{t+\Delta t}}{\Delta t} \tag{3}$$

where *M* is the moisture content (kg water/kg dry matter), *W* is the weight of sample (kg), W_d is the dry matter content of sample (kg), and t is the drying time (min). M_0, M_e, M_t *and* $M_{t+\Delta t}$ are the initial moisture content, the equilibrium moisture content, the moisture content at t and $t+\Delta t$ (kg water/kg dry matter), respectively. As the M_e is very small compared to M_0 and M_t values, the M_e can be neglected and *MR* can be expressed as M_t/M_0 [1].

2.4. Data Analysis

Experimental data were analyzed using the Statistica 8.0.550 (StatSoft Inc., USA) software package. The parameters of the models were estimated using a non-linear regression procedure based on the Levenberg-Marquardt algorithm. The fitting quality of the experimental data to all models was evaluated using the coefficient of determination (R^2), reduced chi-square (χ^2) and root mean square error (*RMSE*). The R^2, χ^2 and RMSE were calculated from the following formulas:

$$R^2 = 1 - \frac{\sum_{i=1}^{N}\left(MR_{pre,i} - MR_{\exp,i}\right)^2}{\sum_{i=1}^{N}\left(\overline{MR}_{pre} - MR_{\exp,i}\right)^2} \tag{4}$$

$$\chi^2 = \frac{\sum_{i=1}^{N}\left(MR_{\exp,i} - MR_{pre,i}\right)^2}{N - z} \tag{5}$$

$$RMSE = \left[\frac{1}{N}\sum_{i=1}^{N}(MR_{pre,i} - MR_{\exp,i})^2\right]^{1/2} \tag{6}$$

where $MR_{exp,i}$ and $MR_{pre,i}$ are the experimental and predicted dimensionless moisture ratios, respectively; N is the number of observations; z is the number of constants. A higher R^2 value and lower χ^2 and $RMSE$ values indicate a better fit [15].

2.5. Calculation of Effective Moisture Diffusivity

Fick's second law of diffusion equation was used to fit the experimental drying data for the determination of effective moisture diffusivity coefficients.

$$\frac{\partial M}{\partial t} = D_{eff}\,\frac{\partial^2 M}{\partial x^2} \tag{7}$$

where M is the moisture content (kg water/kg dry matter), t is the drying time (s), and D_{eff} is the effective moisture diffusivity (m^2/s). The solution of diffusion Eq. (7) for slab geometry is solved by Crank [16] and supposed uniform initial moisture distribution, negligible external resistance, constant temperature and diffusivity, and negligible shrinkage:

$$MR = \frac{8}{\pi^2}\sum_{n=0}^{\infty}\frac{1}{(2n+1)^2}\exp\left(-\frac{(2n+1)^2\pi^2 D_{eff}t}{4L^2}\right) \tag{8}$$

where D_{eff} is the effective moisture diffusivity (m^2/s), L is the half thickness of the slab (m), and n is the positive integer. Eq. (8) can be further simplified to only the first term of the series and expressed in a logarithmic form for long drying periods:

$$\ln(MR) = \ln\left(\frac{8}{\pi^2}\right) - \left(\frac{\pi^2 D_{eff}t}{4L^2}\right) \tag{9}$$

The effective moisture diffusivity was calculated from the slope *(K)* of a straight line, plotting experimental drying data in terms of *ln (MR)* versus *time* according to Eq. (10).

$$K = \frac{\pi^2 D_{eff}}{4L^2} \tag{10}$$

2.6. Estimation of Activation Energy

Temperature was not a directly measurable quantity during the infrared power drying process used in this study. For the calculation of activation energy, modified form of Arrhenius equation shows the relationship between the effective moisture diffusivity and the infrared power to sample weight [17].

$$D_{eff} = D_0 \exp\left(-\frac{E_a\, m}{p}\right) \tag{11}$$

where D_0 is the pre-exponential factor of Arrhenius equation (m^2/s), E_a is the activation energy (W/kg), p is the infrared output power (W), and m is the mass of the product (kg).

2.7. Colour Measurements

The average colour of four different outer surface fresh and dried okra samples were measured by chroma meter (CR-400, Konica Minolta, Tokyo, Japan). The colour values of the samples were expressed as *L* (whiteness / darkness), *a* (redness / greenness), and *b* (yellowness / blueness). The total colour differences (ΔE) and Chroma calculated using Eqs. (12) and (13), respectively:

$$\Delta E = \sqrt{(\Delta L)^2 + (\Delta a)^2 + (\Delta b)^2} \tag{12}$$

$$C = \sqrt{a^2 + b^2} \tag{13}$$

3. RESULTS AND DISCUSSION

3.1. Drying Curves

The effect of infrared power on moisture content and drying time is shown in Figure 1. The infrared power had a significant effect on the moisture content of okra, as expected. It is observed that in infrared drying, an increase in the power level resulted in a decrease at drying time where the required time to reach the final moisture content at the power levels of 62, 74, 88 and 104 W, were about 570, 375, 270 and 210 min, respectively. The average drying rates increased 2.714 times as infrared power increased from 62 W to 104 W. At expected at higher infrared powers the higher heat absorption resulted in higher product temperature, higher mass transfer driving force, faster drying rate and consequently lesser drying. This observation agree well with the results reported in the literature for infrared drying of different products such as pineapple, wormwood and spinach leaves [4,7,18].

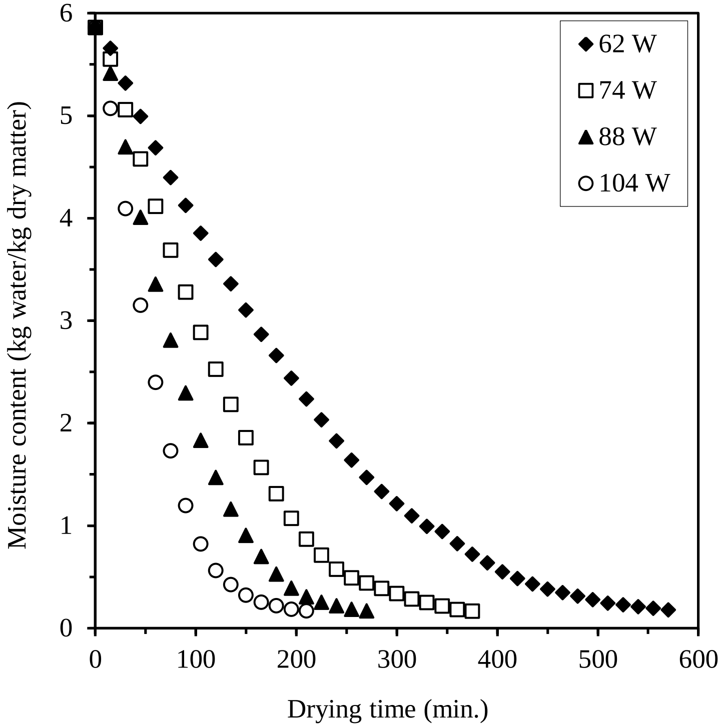

Figure 1. Moisture content versus drying time at different infrared powers

3.2. Drying Rate

The drying rate curves of okra are shown in Figure 2. It is clear that the drying rate decreases continuously with moisture content. The drying rates were higher in the beginning of the process (warming-up period), and then decreased with a decrease in moisture content of the samples. Because the radiation absorptivity of foods increases with an increase in moisture content, thermal energy obtained from infrared radiation was more absorbed by the samples during the initial stage of the process. With the product drying out subsequently, heat penetration though the dried layer decreased, thus retarding the drying rates [4]. In all cases constant drying rate period was not observed and therefore the drying process occurred in the falling drying rate period. These results are in good agreement with those in earlier studies of various vegetables [7,9,18].

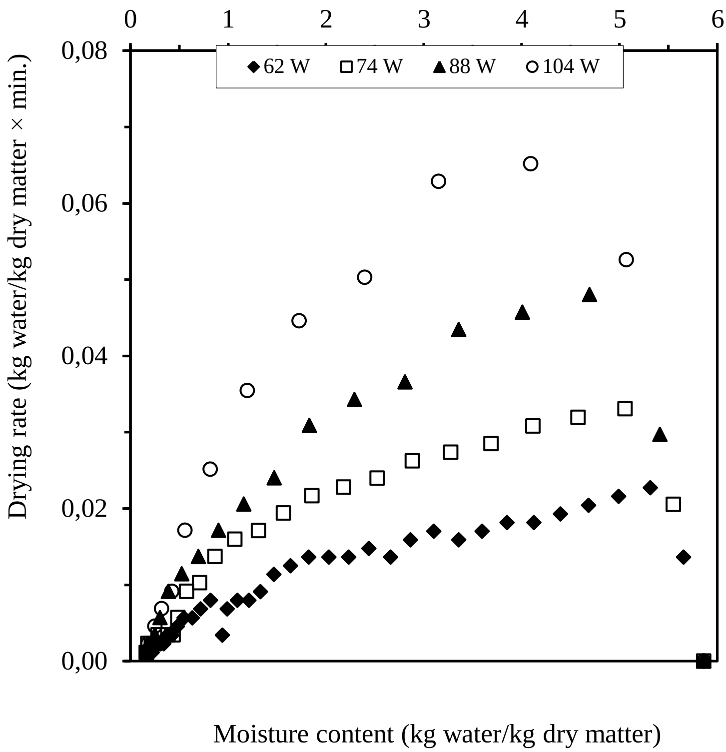

Figure 2. Drying rate as a function of moisture content at different infrared powers

3.3. Evaluation of Models

The moisture content data obtained from the drying experiments were fitted four thin-layer drying models identified in Table 1. The best model selected is based on the highest R^2 and the lowest χ^2 and *RMSE* values. Results of the statistical computing are shown in Table 2. The R^2 values for all models were above 0.98. Among the four thin-layer drying models tested, Midilli & Kucuk model obtained the highest R^2 values and the lowest $\chi^2$and *RMSE* values in all the infrared drying conditions studied. It is clear that, the R^2, χ^2 and *RMSE* values of this model were changed between 0.9994-0.9998, 0.000015-0.000062 and 0.011924-0.033405, respectively. Figure 3 compares experimental data with those predicted with the Midilli & Kucuk model for okra samples. As shown, the predicted moisture ratios are generally banded near to a 45° straight line, indicating the capability of the model to describe the drying behaviour of the samples appropriately.

Table 2. Statistical parameters of models at different infrared powers

Model name	***p (W)***	R^2	χ^2	***RMSE***
Henderson & Pabis	62	0.9897	0.000967	0.168285
	74	0.9861	0.001445	0.163928
	88	0.9872	0.001410	0.134125
	104	0.9877	0.001420	0.114270
Page	62	0.9993	0.000058	0.037277
	74	0.9993	0.000066	0.034381
	88	0.9997	0.000022	0.014546
	104	0.9990	0.000108	0.029022
Midilli & Kucuk	**62**	**0.9996**	**0.000041**	**0.033405**
	74	**0.9994**	**0.000062**	**0.032023**
	88	**0.9998**	**0.000015**	**0.013139**
	104	**0.9998**	**0.000020**	**0.011924**
Aghbashlo et al.	62	0.9989	0.000094	0.048245
	74	0.9970	0.000307	0.074810
	88	0.9969	0.000341	0.059498
	104	0.9956	0.000505	0.069561

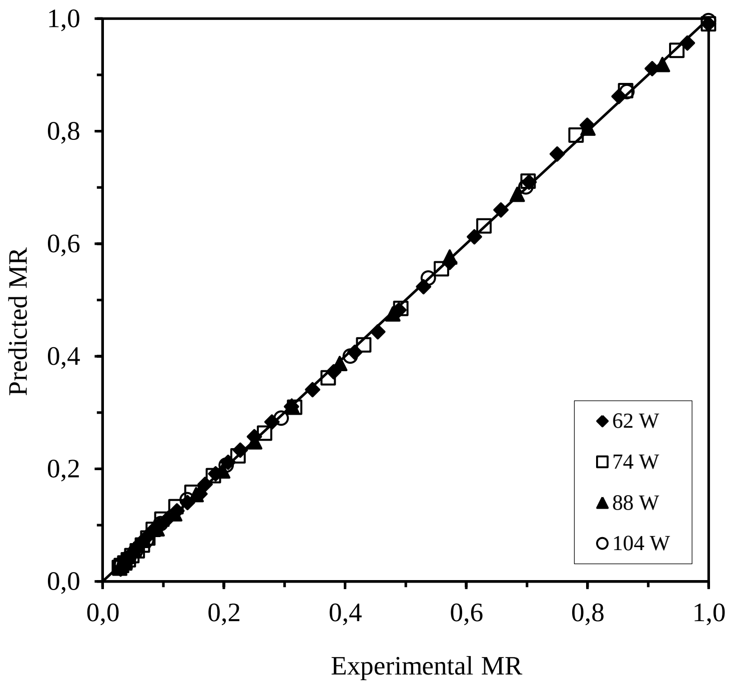

Figure 3. Experimental vs. predicted moisture ratios using Midilli & Kucuk model

3.4. Effective Moisture Diffusivity

By plotting ln (MR) against drying time and using the slope methods the effective moisture diffusivity of the samples was calculated under different drying conditions. The values of effective diffusivity (D_{eff}) were calculated using Eq. (10) and are shown in Figure 4. The D_{eff} values of okra samples in the infrared drying at 62-104 W ranged between 8.54×10^{-10} and 2.32×10^{-9} m^2/s. It can be seen that D_{eff} values increased greatly with increasing infrared power. Drying at 104 W had the highest value of D_{eff} and the lowest value was obtained for 62 W. The values of D_{eff} from this study lie within in general range 10^{-12} to 10^{-8} m^2/s for drying of food materials [19]. The effect of infrared power on effective moisture diffusivity is defined by the following equation:

$$D_{eff} = 5\times10^{-10} p + 3\times10^{-10} \qquad (R^2 = 0.9917) \qquad (14)$$

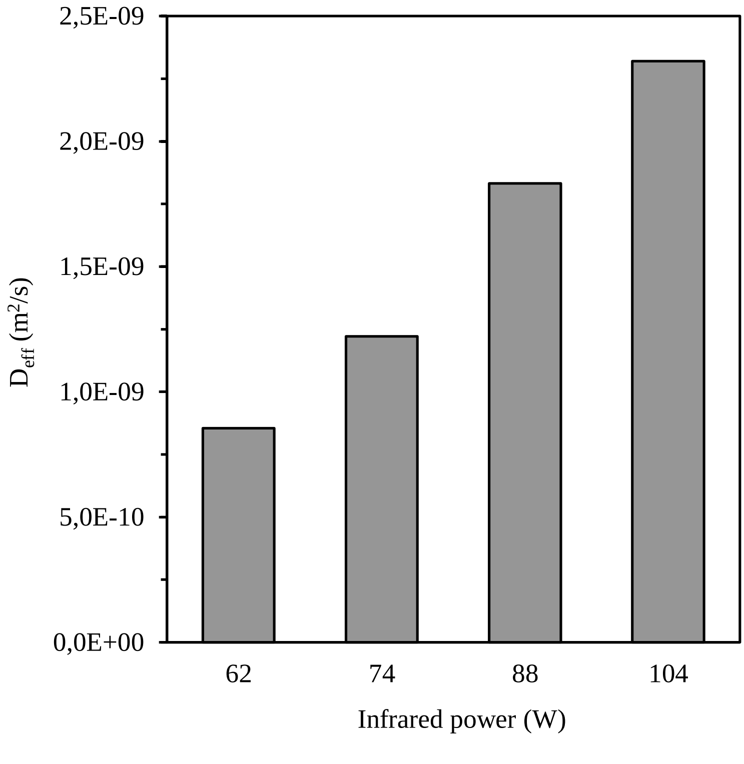

Figure 4. Variation of effective moisture diffusivity with infrared powers

3.5. Activation Energy

The activation energy can be determined from the slope of Arrhenius plot, *ln* (D_{eff}) versus *m/p* (Eq. (11)). The *ln* (D_{eff}) as a function of the sample weight/infrared power was plotted in Figure 5. The slope of the line is ($-E_a$) and the intercept equals to ln (D_0). The results show a linear relationship due to Arrhenius type dependence. Eq. (15) shows the effect of sample weight/infrared power on D_{eff} of samples with the following coefficients:

$$D_{eff} = 1.053 \times 10^{-8} \exp\left(-\frac{3915.1\ m}{p}\right) \qquad (R^2 = 0.9954) \qquad (15)$$

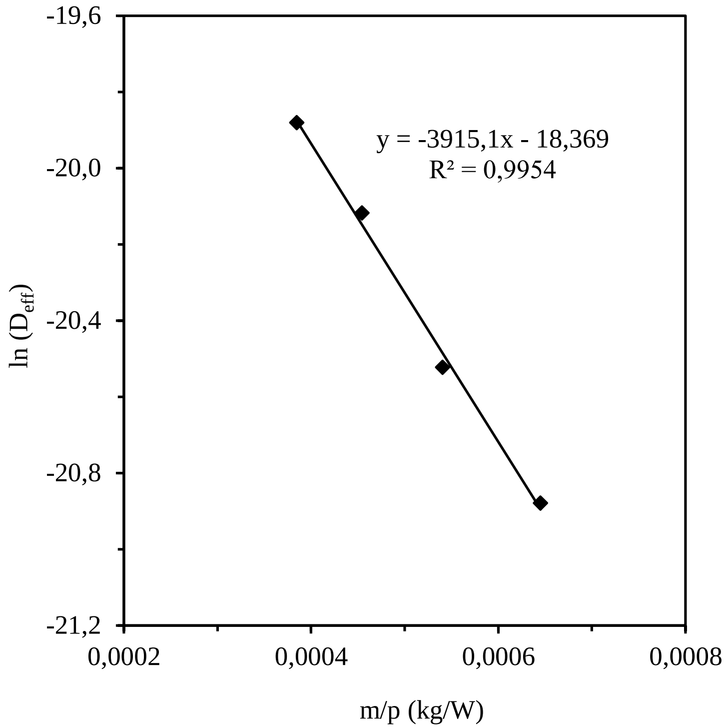

Figure 5. Arrhenius-type relationship between effective moisture diffusivity and infrared powers

The estimated values of D_0 and E_a from modified Arrhenius type exponential Eq. (15) are 1.053×10^{-8} m^2/s and 3.91 kW/kg, respectively.

3.6. Colour

Colour is one of the most important quality attributes that influences the general acceptability of consumers [14]. The colour values of fresh okras were measured as *L*, *a*, and *b* equal to 43.90±0.25, -4.74±0.03, and 9.85±0.08, respectively. Table 3 represents *L*, *a*, *b*, *ΔE*, and *C* average values and standard deviations of dried okra samples. The obtained results from Table 3 for colour measurement at various conditions indicated that infrared power has a considerable effect on the colour parameters. *L* and *b* values of dried samples decreased as the infrared power increased. In contrast, as the infrared power increased, the *a* values increased. With respect to presented results in Table 3, the *L* values changed from 43.04±0.26 to 40.78±0.19 at various drying conditions. The decrease in L values can be attributed to brown pigment formation during drying process due to the high levels of reducing sugars and amino acids in okra slices. Similar study was reported by Pathare et al. [20]. The changes in *b* value may be due to decomposition of chlorophyll and carotenoid pigments, non-enzymatic Maillard browning and formation of brown pigments. With increasing in IR power from 62 to 104 W, ΔE was increased from 11.04±0.11 to 12.57±0.13, respectively. Aidani et al. [21] found that high temperature is responsible for increasing ΔE values during drying of kiwifruit slices. The chroma is measure of chromaticity (C), which denotes the purity or saturation of the colour [22]. The chroma (C) values showed a decrease during process. Chroma (C) values varied from 7.65±0.08 to 7.10±0.07 at different IR powers and showed a decrease as the IR power increased.

Table 3. Results of colour values for okra samples

p (W)	***L***	***a***	***b***	***ΔE***	***C***
62	43.04±0.26	5.36±0.05	5.47±0.06	11.04±0.11	7.65±0.08
74	41.36±0.24	5.70±0.06	4.35±0.04	12.07±0.12	7.17±0.07
88	41.28±0.23	5.81±0.07	4.17±0.04	12.26±0.12	7.15±0.07
104	40.78±0.19	5.91±0.07	3.94±0.03	12.57±0.13	7.10±0.07

4. CONCLUSIONS

Based on the experimental tests reported in this study, it is observed that the infrared power significantly affects the drying and colour characteristics of dried okra. Drying time decreased considerably with increase in infrared power. The drying was observed to take place entirely in the falling-rate drying period and hence moisture migration to the surface is based on diffusion. To explain the drying kinetics of okra samples, four mathematical models were applied and fitted to the experimental data. According to the results of statistical analysis, the experimental data were well predicted by the Midilli & Kucuk model. The effective moisture diffusivity increased as infrared power increased. The colour values of *a* and ΔE increased while those of *L*, *b* and *C* decreased as the power output increased.

REFERENCES

[1] Li, H., Xie, L., Ma, Y., Zhang, M., Zhao, Y., Zhao, X., (2019), Effects of drying methods on drying characteristics, physicochemical properties and antioxidant capacity of okra, *LWT - Food Science and Technology* 101, 630-638.

[2] FAO, (2018), http://www.fao.org/faostat/en/#data/QC (Updated May 28, 2018).

[3] Tüfekçi S., Özkal S.G., (2017), Enhancement of drying and rehydration characteristics of okra by ultrasound pre-treatment application, *Heat and Mass Transfer* 53, 2279-2286.

[4] Beigi M., (2018)., Effect of infrared drying power on dehydration characteristics, energy consumption, and quality attributes of common wormwood (*Artemisia absinthium* L.) leaves, *Journal of Agricultural Science and Technology* 20, 709-718.

[5] Riadh M.H., Ahmad S.A.B., Marhaban M.H., Soh A.C., (2015), Infrared heating in food drying: An overview, *Drying Technology* 33, 322-335.

[6] Nowak D., Lewicki P.P., (2004), Infrared drying of apple slices, *Innovative Food Science & Emerging Technologies* 5, 353-360.

[7] Ponkham K., Meeso N., Soponronnarit S., Siriamornpun S., (2012), Modeling of combined far-infrared radiation and air drying of a ring shaped-pineapple with/without shrinkage, *Food and Bioproducts Processing* 90, 155-164.

[8] Corrêa P.C., de Oliveira G.H.H., Baptestini F.M., Diniz M.D.M.S., da Paixão A.A., (2012), Tomato infrared drying: Modeling and some coefficients of the dehydration process, *Chilean Journal of Agricultural Research* 72, 262-267.

[9] Doymaz I., (2017), Infrared drying characteristics of Jerusalem artichoke slices, *Sigma Journal of Engineering and Natural Sciences* 35, 227-238.

[10] Falade K.O., Omojola B.S., (2010), Effect of processing methods on physical, chemical, rheological, and sensory properties of okra (*Abelmoschus esculentus*), *Food and Bioprocess Technology*, 387-394.

[11] Afolabi T.J., (2014), Thin layer drying kinetics and modelling of okra (*Abelmoschus esculentus* (L.) Moench) slices under natural and forced convective air drying, *Food Science and Quality Management* 28, 35-49.

[12] Doymaz I., (2011), Drying of green bean and okra under solar energy, *Chemical Industry & Chemical Engineering Quarterly* 17, 199-205.

[13] Ismail M.A., Ibn Idriss, E.M., (2013), Mathematical modelling of thin layer solar drying of whole okra (*Abelmoschus esculentus* (L.) Moench) pods, International Food Research Journal 20, 1983-1989.

[14] Huang J., Zhang M., (2016), Effect of three drying methods on the drying characteristics and quality of okra, Drying Technology 34, 900-911.

[15] Chayjan R.A., Salari K., Abedi Q., Sabziparvar A.A., (2013), Modeling moisture diffusivity, activation energy and specific energy consumption of squash seeds in a semi fluidized and fluidized bed drying, *Journal of Food Science and Technology* 50, 667-677.

[16] Crank J., (1975), The Mathematics of Diffusion, Oxford University Press, London, UK.

[17] Darvishi H., (2017), Quality, performance analysis, mass transfer parameters and modeling of drying kinetics of soybean. *Brazilian Journal of Chemical Engineering* 34, 143-158.

[18] Sarimeseli A., Yuceer M., (2015)., Investigation of infrared drying behaviour of spinach leaves using ANN methodology and dried product quality, *Chemical and Process Engineering* 36, 425-436.

[19] Zogzas N.P., Maroulis Z.B., Marinos-Kouris D., (1996)., Moisture diffusivity data compilation in foodstuffs, *Drying Technology* 14, 2225-2253.

[20] Pathare, P.B., Opara, U.L., Al-Said, F.A.J., (2013), Colour measurement and analysis in fresh and processed foods: A review, *Food and Bioprocess Technology* 6, 36-60.

[21] Aidani E., Hadadkhodaparast M., Kashaninejad M., (2017), Experimental and modeling investigation of mass transfer during combined infrared-vacuum drying of Hayward kiwifruits, *Food Science & Nutrition* 5, 596–601.

[22] Salehi F., Kashaninejad M., (2015), Effect of drying methods on rheological and textural properties, and color changes of wild sage seed gum, *Journal of Food Science and Technology* 52, 7361-7368.